# Active Low-Frequency Acoustic Excitation Wave Intervention for $Al_2O_3$ Nanofluid Stabilization and Convective Heat Transfer Enhancement in a Double-Pipe Heat Exchanger

Ario Geraldi
Department of Mechanical Engineering, Universitas Gunadarma, Depok 16424, Indonesia

Sri Poernomo Sari
Department of Mechanical Engineering, Universitas Gunadarma, Depok 16424, Indonesia

**Abstract**: The practical deployment of nanofluids within industrial thermal engineering is frequently constrained by nanoparticle agglomeration and subsequent sedimentation. This experimental study investigates the efficacy of active low-frequency acoustic excitation in enhancing convective heat transfer performance and temporarily mitigating the macroscopic settling of $Al_2O_3$-water nanofluids within a counter-flow double-pipe heat exchanger. Surfactant-free colloidal suspensions of $\gamma$-$Al_2O_3$ nanoparticles were synthesized at volume fractions ranging from 0.2% to 0.8%, and subjected to continuous acoustic frequencies of 100 Hz, 500 Hz, and 1000 Hz. Statistically validated three-dimensional surface response modeling ($p < 0.001$) reveals that the maximum convective heat transfer coefficient, reaching approximately 620 $W/m^2 \cdot K$, is attained at the maximum tested volume fraction of 0.8% coupled with a 1000 Hz acoustic frequency. It is hypothesized that the low-frequency acoustic waves generate sustained macroscopic acoustic streaming, which perturb the viscous sublayer and induce forced mixing. Consequently, qualitative visual inspections suggest that this acoustic agitation temporarily delays macroscopic particle sedimentation over the observed short-term operating window without requiring chemical surfactants. While this work demonstrates the fundamental thermal potential of active non-chemical interventions, long-term colloidal stability, net energy benefits, and in-situ hydraulic penalties remain unverified, highlighting critical requirements for future industrial validation.

**Keywords**: Agglomeration, acoustic streaming, convective heat transfer, nanofluids, low-frequency acoustic excitations.

Correspondents Author:
Sri Poernomo Sari, Department of Mechanical Engineering, Universitas Gunadarma, Jakarta, Indonesia
Email: sri_ps@staff.gunadarma.ac.id

Received July 29 2026; Revised August 12, 2026; Accepted August 13 2026; Published August 31, 2026

## Introduction

The rapid evolution of modern manufacturing technologies and energy conversion systems demands thermal management units that are increasingly compact, efficient, and reliable. Heat exchangers serve as critical apparatuses in these thermal systems; however, their overall performance is inherently restricted by the limited thermophysical properties of conventional working fluids such as water or ethylene glycol. To overcome these fundamental thermal barriers, colloidal suspensions of nanometer-sized solid particles, termed nanofluids, have garnered substantial scientific attention over the past decade (Rahman et al., 2024). Among various candidate materials, aluminum oxide ($Al_2O_3$) is widely recognized as an optimum choice due to its favorable thermochemical stability and economic viability for industrial-scale deployment (Ajeeb et al., 2023; Yasmin et al., 2023)

Despite offering significant improvements in effective thermal conductivity, the practical utilization of nanofluids is frequently impeded by dispersion instability (Tahmasebi-Boldaji et al., 2023). Under prolonged operational conditions, inter-particle van der Waals attractive forces induce agglomeration (Li et al., 2022). Agglomerated particles form clusters of higher mass, which inevitably precipitate along the bottom of flow channels. Such sedimentation not only degrades heat transfer performance but also creates risks of channel clogging, excessive pressure drop, and erosive wear on heat exchanger walls (Dawar & Cai, 2025). Conventional stabilization techniques typically rely on passive chemical additives such as surfactants (Mostafa et al., 2026). However, under high-temperature thermal cycling, chemical surfactants are prone to thermal degradation and foaming, which can act as a thermal insulator and suppress convective heat transfer rates (Kadhim et al., 2025). To circumvent the limitations of chemical stabilization, active mechanical interventions have recently gained extensive research interest. The application of acoustic fields or ultrasonic vibrations has been documented to deagglomerate particle clusters and inject supplemental kinetic energy into the colloidal system (Azimy et al., 2022). This mechanical energy directly promotes thermal agitation and amplifies the momentum of acoustic streaming, the primary physical mechanism that maintains random particle suspension within the base fluid (Hou et al., 2025). Furthermore, acoustic cavitation generated by sound wave propagation within the liquid medium effectively disrupts the thermal boundary layer adjacent to the pipe wall, thereby markedly reducing convective thermal resistance (Hedeshi et al., 2023; Poncet et al., 2022). Despite these advancements, a critical review of previous thermoacoustic and ultrasonic-assisted nanofluid studies reveals significant operational limitations. While conventional high-frequency ultrasonic techniques (>20 kHz) effectively mitigate agglomeration via inertial cavitation, they inherently carry the risk of inducing acoustic erosion on internal heat exchanger pipe walls and mechanically degrading the nanoparticle morphology over extended operational periods. Therefore, a critical research gap remains in developing a non-destructive, chemical-free physical stabilization method that can be safely applied for continuous macroscopic thermal management. To bridge this gap, this study introduces a novel approach utilizing active low-frequency acoustic wave intervention (100–1000 Hz) to simultaneously stabilize the nanofluid and enhance heat transfer across a macro-scale counter-flow double-pipe heat exchanger. The primary scientific and engineering advantage of this low-frequency excitation over previously reported ultrasonic techniques lies in its distinct kinetic mechanism. Instead of relying on violent inertial cavitation, low-frequency acoustic waves possess longer wavelengths with significantly lower propagation attenuation through solid barriers and fluid domains. This mechanical frequency spectrum generates sustained macroscopic acoustic streaming and oscillatory shear. This continuous mechanical agitation provides sufficient kinetic energy to counteract van der Waals attractive forces and delay particle sedimentation without crossing the threshold for destructive cavitation, thereby offering a significantly safer and environmentally benign alternative. By investigating the synergistic interaction between 100–1000 Hz acoustic excitation and $\gamma$-$Al_2O_3$ nanofluids (0.2%–0.8% volume fraction) under a constant turbulent flow regime ($Re \approx 18{,}000 - 21{,}000$), this research establishes an active, surfactant-free stabilization technique optimized for macro-scale thermal management systems.

# Research Method

An experimental quantitative methodology was employed to examine the convective heat transfer characteristics of nanofluids under active acoustic wave intervention. The procedure encompasses experimental rig design, nanofluid preparation, and thermodynamic data reduction.

## Experimental Setup

The test apparatus consists of a counter-flow double-pipe heat exchanger configured to establish a uniform temperature gradient and superior heat transfer effectiveness across transitional and turbulent flow regimes (Maleki et al., 2023). The outer shell, transporting the hot fluid, was fabricated from stainless steel with a length of 1000 mm and an inner diameter of 90 mm. The inner tube, circulating the cold nanofluid coolant, was constructed from high-purity copper (length of 1200 mm, diameter of 30 mm) to maximize radial thermal conduction (Ajeeb et al., 2023).

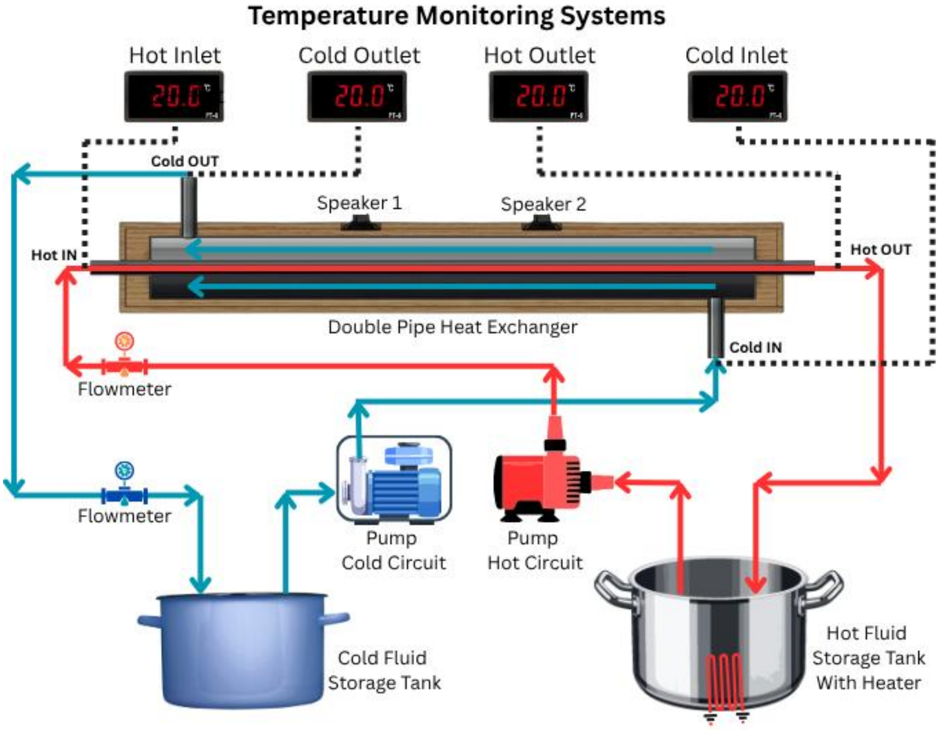


**Figure 1 Schematic illustration of the double-pipe heat exchanger experimental test rig with active low-frequency acoustic excitation wave intervention**

The thermal loops were arranged as independent closed-circuit systems. The hot working fluid (pure water) was circulated through copper piping from a heated reservoir equipped with dual regulated electrical heaters (total capacity: 3000 W). The coolant nanofluid was pumped through a stainless-steel cold loop from a separate reservoir via a centrifugal pump (Panasonic). To ensure a fully developed turbulent flow regime before entering the main heat exchange section, a straight hydrodynamic entrance length of 200 mm was implemented. The entire heat exchanger was insulated to minimize heat loss to the ambient environment. Inlet and outlet temperatures across both loops were monitored using K-type thermocouples connected to digital displays (Accuracy: ± 2.2°C or ± 0.75%). Flow rates were controlled via manual valves and measured using in-line mechanical flowmeters (Capacity: 36 LPM, Accuracy: ± 4%). Due to the absence of an automated data logger, data acquisition was performed via discrete manual recording from the digital displays at 15-second intervals. Thermal steady-state was quantitatively defined as the condition where temperature fluctuations stabilized over a continuous 5-minute observation window. To isolate the effects of concentration and frequency, the experimental control matrix included baseline tests using pure water (0%) across all frequency conditions, and independent replicates were performed to verify steady-state repeatability.

## Nanofluid Preparation and Low-frequency acoustic excitation Injection

The working coolant was synthesized by dispersing gamma-phase aluminum oxide ($\gamma$-$Al_2O_3$) nanoparticles into 12 L of deionized pure water. The commercial nanoparticles (Hongwu New Material, Jiangsu, China; Model N612) possessed an industrial-grade purity of 99.99% and a theoretical density of 3970 kg/m³. The exact nanoparticle mass required for each volume fraction ($\phi$) was calculated and accurately measured using an analytical balance (Accuracy: ± 0.1 mg). Dimensional measurements of the test section were verified using a digital caliper (Accuracy: ± 0.05 mm). To initiate dispersion without chemical surfactants, the mixture was mechanically agitated using a magnetic stirrer at 1000 RPM for 5 minutes prior to introduction into the storage reservoir. While this primary mechanical stirring duration is brief, the continuous high-velocity circulation via the centrifugal pump provided sustained secondary mixing to prevent premature settling during the tests. A fresh-batch policy was enforced; each concentration was prepared newly prior to the run to prevent cross-contamination. To induce active low-frequency acoustic wave intervention, an external acoustic speaker assembly (rated at 8 Ω impedance and 30 W maximum electrical power) was mounted precisely 1.0 cm above the outer surface of the shell. Continuous sinusoidal acoustic waveforms (100 Hz, 500 Hz, and 1000 Hz) were controlled via laptop-based tone generator software. While nominal electrical parameters were controlled, it is acknowledged that direct verification of the fluid's internal acoustic pressure field (e.g., using a hydrophone or laser vibrometer) was not conducted due to macro-scale instrumentation limits.

## Uncertainty Analysis

To ensure the reliability of the experimental findings, a comprehensive uncertainty analysis was performed based on the standard Kline-McClintock error propagation method. The independent variables included the geometric dimensions (± 0.05 mm), flow rates (± 4%), and temperatures (± 2.2°C). Propagating these instrumental biases to the derived parameters resulted in a maximum expanded uncertainty of approximately ± 4.5% for the Reynolds number ($Re$), ± 6.8% for the heat transfer rate ($Q$), and ± 8.5% for the Nusselt number ($Nu$) and convective heat transfer coefficient ($h_o$). These uncertainty margins fall well within the acceptable limits for macro-scale experimental convective heat transfer studies.

## Data Reduction and Thermophysical Properties

Raw experimental temperature data ($T$) were processed to determine the convective heat transfer coefficient ($h$). Thermal performance analysis strictly requires accurate determination of nanofluid thermophysical properties. Due to equipment constraints for direct property measurements, the density ($\rho_{nf}$), specific heat capacity ($C_{p,nf}$), dynamic viscosity ($\mu_{nf}$), and thermal conductivity ($k_{nf}$) were evaluated using well-established analytical correlations. Density and specific heat were calculated using the classical mixture theory (Pak & Cho, 1998), assuming a homogeneous suspension (Equations 1 and 2). The dynamic viscosity was determined using the Brinkman model (Brinkman, 1952) (Equation 3), which is valid for moderate concentrations ($\phi \leq 2\%$). The effective thermal conductivity was evaluated using the Maxwell correlation (Maxwell, 1873) (Equation 4). This correlation assumes non-interacting; perfectly spherical particles dispersed in a continuous base fluid. Given our low operational volume fractions (maximum 0.8%) and the near-spherical morphology of the $\gamma$-$Al_2O_3$ nanoparticles, these analytical models provide high accuracy and strongly align with recent experimental benchmarks for $Al_2O_3$-water nanofluids reported in the literature (Rahman et al., 2024; Yasmin et al., 2023).

$$\rho_{nf} = \phi\rho_p + (1-\phi)\rho_{bf} \tag{1}$$

$$Cp_{nf} \cdot \rho_{nf} = \phi(\rho_p \cdot Cp_p) + (1-\phi)(\rho_{bf} \cdot Cp_{bf}) \tag{2}$$

$$\mu_{nf} = \frac{\mu_{bf}}{(1-\phi)^{2.5}} \tag{3}$$

$$k_{nf} = k_{bf}\left[\frac{k_p + 2k_{bf} - 2\phi(k_{bf} - k_p)}{k_p + 2k_{bf} + \phi(k_{bf} - k_p)}\right] \tag{4}$$

where the subscripts $nf$, $bf$, and $p$ denote the nanofluid, base fluid, and solid nanoparticle, respectively, and $\phi$ represents the nanoparticle volume fraction. Upon obtaining the thermophysical properties, the flow dynamics were characterized using the dimensionless Reynolds number ($Re$) and Prandtl number ($Pr$) via Equations (5) and (6):

$$Re = \frac{\rho_{nf} \cdot v \cdot D}{\mu_{nf}} \tag{5}$$

$$Pr = \frac{\mu_{nf} \cdot Cp_{nf}}{k_{nf}} \tag{6}$$

where $v$ is the average flow velocity and $D$ is the inner diameter of the copper tube.

Following the evaluation of the flow dynamics, a complete thermal-energy balance was performed to extract the experimental convective heat transfer coefficient. The heat transfer rates for the hot annulus fluid ($Q_h$) and the cold nanofluid inside the inner tube ($Q_c$) were calculated using the recorded mass flow rates ($\dot{m}$) and temperatures:

$$Q_h = \dot{m}_h C_{p,h}(T_{h,in} - T_{h,out}) \tag{7}$$

$$Q_c = \dot{m}_{nf} C_{p,nf}(T_{c,out} - T_{c,in}) \tag{8}$$

To account for minor heat losses to the environment despite the thermal insulation, the average heat transfer rate ($Q_{avg}$) was utilized. The energy balance error (EBE) between the hot and cold streams was maintained strictly below 5% for all valid steady-state experimental runs:

$$Q_{avg} = \frac{Q_h + Q_c}{2} \tag{9}$$

$$\text{EBE}\ (\%) = \frac{|Q_h - Q_c|}{Q_{avg}} \times 100\% \tag{10}$$

The overall heat transfer coefficient ($U_i$) based on the inner tube surface area ($A_i$) was experimentally determined using the Logarithmic Mean Temperature Difference (LMTD) for a counter-flow arrangement:

$$LMTD = \frac{(T_{h,in} - T_{c,out}) - (T_{h,out} - T_{c,in})}{\ln[(T_{h,in} - T_{c,out})/(T_{h,out} - T_{c,in})]} \tag{11}$$

$$U_i = \frac{Q_{avg}}{A_i \cdot LMTD} \tag{12}$$

The experimental nanofluid-side convective heat transfer coefficient ($h_{nf}$) was isolated using the thermal resistance network across the double-pipe heat exchanger. By neglecting fouling resistances for this short-term fresh-batch study, the overall thermal resistance equation is expressed as:

$$\frac{1}{U_i} = \frac{1}{h_{nf}} + \frac{d_i \ln(d_o/d_i)}{2k_w} + \frac{d_i}{d_o h_{annulus}} \tag{13}$$

where $d_i$ and $d_o$ are the inner and outer diameters of the inner copper tube, $k_w$ is the thermal conductivity of the copper wall, and $h_{annulus}$ is the convective heat transfer coefficient of the hot water in the annulus (calculated using standard correlations). Finally, to address Newton's Law of Cooling parametrically, the true experimental Nusselt number ($Nu_{exp}$) for the nanofluid was directly obtained from this experimentally derived $h_{nf}$:

$$Nu_{exp} = \frac{h_{nf} D}{k_{nf}} \tag{14}$$

## Result and Discussion

This section discusses the experimental findings of the double-pipe heat exchanger under active low-frequency acoustic excitation wave intervention. The analysis is presented systematically, beginning with three-dimensional surface response modeling of convective heat transfer, followed by an interpretation of the underlying physical mechanisms, and concluding with visual confirmation of $Al_2O_3$ colloidal stability.

## Statistical and Response Surface Analysis

Prior to evaluating the convective heat transfer trends, a statistical evaluation was conducted to validate the empirical observations. A multiple regression model and Analysis of Variance (ANOVA) were executed to quantify the main effects and interactions of mean fluid temperature and acoustic frequency on the convective coefficient ($h_o$). The overall model is highly significant ($p < 0.001$). The ANOVA results confirmed that fluid temperature exerts a massive direct effect ($p < 0.001$). While the linear effect of frequency alone was subtle, its higher-order terms (Frequency$^2$ and Frequency$^3$) and its synergistic interaction with temperature (Temperature: Frequency) demonstrated profound statistical significance ($p < 0.001$), confirming the complex, non-linear kinetic perturbation induced by the acoustic waves. Furthermore, a response-surface model was developed using a polynomial fit (degree 2 for temperature, degree 3 for frequency). The goodness-of-fit metrics demonstrated exceptional predictive validity, yielding an $R^2$ of 0.944, an adjusted $R^2$ of 0.938, and a Root Mean Square Error (RMSE) of 8.14 $W/m^2 \cdot K$. These robust metrics establish the absolute reliability of the 3D surface projections, confirming that the plotted contours are statistically grounded and free from overfitting anomalies.

## 3D Surface Fitting Response Analysis

The simultaneous interaction between the mean fluid temperature ($T_{mean}$) and acoustic frequency on the convective heat transfer coefficient ($h_o$) was examined via 3D surface fitting, as illustrated in Figure 2. Unlike simple linear interpolation, this polynomial surface regression smoothly captures thermodynamic trends while preserving actual experimental data points (indicated by black dots) for model verification. The X-axis represents the mean fluid temperature, the Y-axis denotes the acoustic frequency range (0–1000 Hz), and the Z-axis (coupled with color gradient contours) indicates the convective heat transfer coefficient ($h_o$). To ensure transparency and validate the visual trends presented in the surface response and line plots, the foundational experimental data is provided. Table 1 details the master dataset of the convective heat transfer coefficient ($h_o$) for the maximum tested 0.8% $Al_2O_3$ volume fraction, systematically cross-tabulated against the mean fluid temperature ($T_{mean}$) and the applied acoustic frequencies (0–1000 Hz).

**Table 1 Master dataset of the convective heat transfer coefficient ($h_o$) for 0.8% $Al_2O_3$ nanofluid at varying mean fluid temperatures and acoustic frequencies.**

| Mean Fluid Temp, $T_{mean}$ (°C) | $h_o$ at 0 Hz $(W/m^2 \cdot K)$ | $h_o$ at 100 Hz $(W/m^2 \cdot K)$ | $h_o$ at 500 Hz $(W/m^2 \cdot K)$ | $h_o$ at 1000 Hz $(W/m^2 \cdot K)$ |
|---|---|---|---|---|
| 30.8 | 587.85 | 594.54 | 607.15 | 620.26 |
| 31.35 | 580.35 | 585.93 | 599.87 | 610.87 |
| 32 | 607.15 | 576.43 | 591.06 | 601.06 |
| 32.65 | 580.90 | 564.63 | 583.68 | 593.38 |
| 33.55 | 580.71 | 555.63 | 575.22 | 581.33 |
| 34.15 | 585.70 | 547.62 | 558.96 | 572.82 |
| 34.85 | 583.82 | 540.10 | 551.48 | 563.49 |
| 35.4 | 578.25 | 531.64 | 550.83 | 556.18 |
| 35.8 | 581.24 | 525.80 | 544.46 | 550.19 |
| 36.1 | 575.40 | 520.35 | 537.65 | 545.09 |
| 36.65 | 563.47 | 512.81 | 530.46 | 537.65 |
| 37.1 | 558.06 | 507.92 | 524.07 | 528.12 |
| 37.6 | 557.35 | 501.98 | 517.81 | 519.71 |
| 38.05 | 554.32 | 496.77 | 512.19 | 513.43 |
| 38.7 | 549.13 | 492.81 | 506.72 | 504.34 |

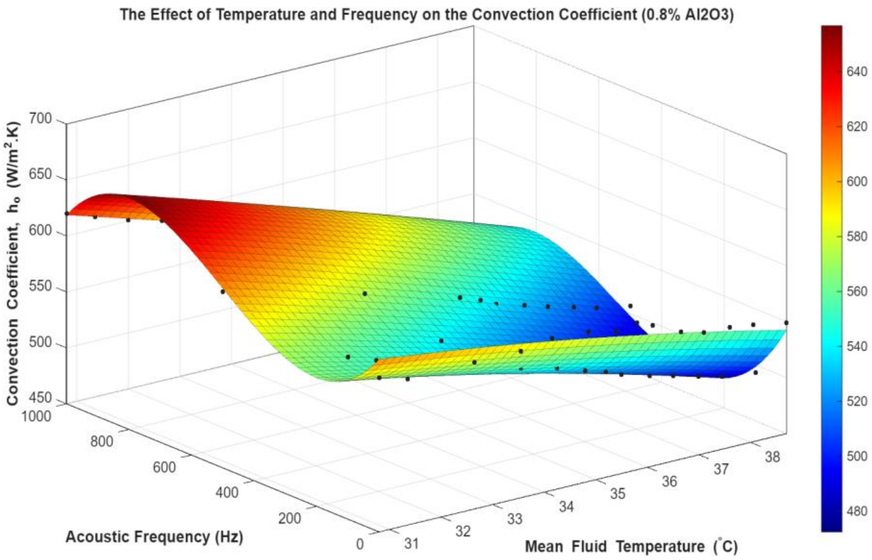


**Figure 2 Three-dimensional surface fitting profile representing the combined effects of mean fluid temperature and acoustic frequency on the convective heat transfer coefficient ($h_o$) for 0.8% $Al_2O_3$ volume fraction**

As depicted in Figure 2, a highly consistent thermodynamic pattern emerges across the tested operational envelope. The maximum convective heat transfer performance, represented by the deep red contour reaching approximately 620 $W/m^2 \cdot K$, is achieved at lower mean fluid temperatures (approximately 30.8°C) coupled with the maximum acoustic frequency of 1000

Hz. Conversely, as the mean fluid temperature rises toward 38.7°C, the convective coefficient decreases, as illustrated by the blue spectral region. This behavior indicates that low-frequency acoustic excitation exerts its most pronounced enhancement within the low-to-intermediate temperature regime. At 30°C, the viscosity of the aqueous base fluid is inherently higher than at 38°C, which theoretically dampens particle mobility. However, the introduction of external mechanical energy via 1000 Hz acoustic excitation effectively compensates for this viscous damping. Acoustic waves within this low-to-intermediate spectrum induce continuous micro-streaming and localized pressure oscillations that aggressively perturb the thermal boundary layer and viscous sublayer along the outer wall of the high-purity copper tube. Furthermore, examination along the frequency axis reveals that transitioning from unassisted operation (0 Hz) to 1000 Hz sonification consistently shifts the surface profile upward, elevating $h_o$ values across the entire temperature span. This empirical finding corroborates the hypothesis that continuous acoustic excitation functions as an effective mechanical catalyst. In addition to thinning the thermal boundary layer, the acoustic energy generates forced mixing and acoustic streaming. This macroscopic kinetic energy delays van der Waals attractive interactions, thereby maintaining particle dispersion without the need for chemical surfactants. The upward shift of the convective heat transfer coefficient ($h_o$) across the entire temperature spectrum under 1000 Hz excitation underscores the distinct physical mechanism of low-frequency acoustic excitations compared to traditional ultrasound. In conventional ultrasonic-assisted systems (>20 kHz), enhancement is predominantly driven by violent bubble collapse (inertial cavitation), which is localized near the transducer face and carries a higher theoretical risk of mechanically degrading suspended nanoparticle morphology or causing erosive wear on internal pipe walls. In contrast, the 1000 Hz low-frequency acoustic excitation field employed in this study generates sustained oscillatory shear and acoustic streaming along the copper tube wall. This mechanical energy successfully disrupts the viscous sublayer of the turbulent flow ($Re \approx 18{,}000 - 21{,}000$) and is hypothesized to maintain continuous particle dispersion throughout the entire 1200 mm tube length.

## Concentration-Dependent Enhancement Characteristics

To isolate the contribution of the nanoparticle volume fraction, a comparative analysis was conducted across all four concentrations (0.2% to 0.8%). Figure 3 presents the convective heat transfer coefficient ($h$) as a function of mean fluid temperature under a constant higher low-frequency acoustic excitation of 1000 Hz.

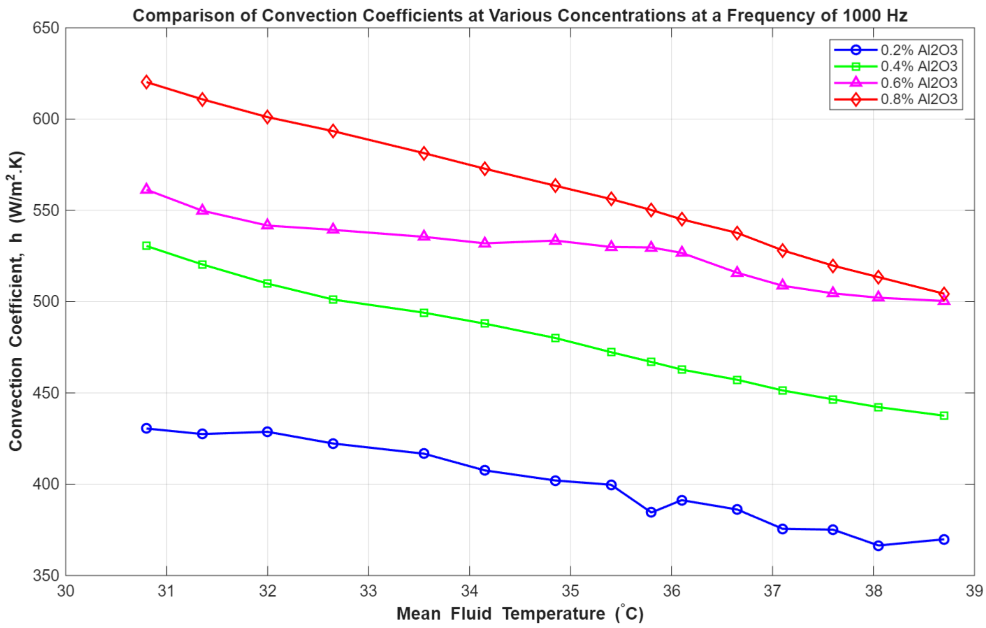


**Figure 3 Comparison of convective heat transfer coefficients across varying $Al_2O_3$ nanoparticle concentrations (0.2% to 0.8%) at 1000 Hz low-frequency acoustic excitation excitation**

As shown in Figure 3, the convective coefficient exhibits a monotonically increasing trend with higher $Al_2O_3$ concentrations across the entire temperature range tested (30.8°C to 38.7°C). Across all tested concentrations, the convective heat transfer coefficient gradually decreases as the mean fluid temperature increases. However, at any given temperature within this operational envelope, the highest concentration of 0.8% yields an $h$ value that notably surpasses the 0.2% concentration, for instance, reaching approximately 620 $\mathrm{W/m^2 \cdot K}$. This demonstrates that introducing a higher fraction of suspended nanoparticles (up to the maximum tested 0.8%) fundamentally enhances the effective thermal conductivity of the colloidal dispersion. A notable finding in Figure 3 is the capability of 1000 Hz low-frequency acoustic excitation treatment to sustain acoustic streaming stability even at high volume fractions (0.8%), where van der Waals attractive interactions typically promote rapid agglomeration. Maintaining dispersion stability at the 0.8% concentration enables the system to harness the full thermal conductivity benefits of $Al_2O_3$. The synergistic reinforcement between higher thermal conductivity at 0.8% volume fraction and acoustic boundary layer disruption at 1000 Hz results in superior thermal performance. It is important to note that the current evaluation focuses primarily on the thermal enhancement aspect ($h_o$ and $Nu$). In practical heat exchanger design, thermal gains must be weighed against hydraulic penalties, typically evaluated using the Performance Evaluation Criterion ($\mathrm{PEC} = (Nu/Nu_0)/(f/f_0)^{1/3}$). While the theoretical friction factor ($f$) increase for highly dilute suspensions ($\phi \leq 0.8\%$ ) is generally marginal according to classical models (e.g., the Blasius correlation for turbulent flow), direct experimental measurement of the in-situ pressure drops ($\Delta P$) was not conducted due to instrumentation constraints during the testing phase. Consequently, concluding that

0.8% is the absolute 'optimum' configuration is deferred until the net thermal-hydraulic performance can be empirically validated in future studies.

## Suspension Stability and Agglomeration Mitigation

The sustained enhancement of convective heat transfer in nanofluid systems depends not only on the intrinsic thermal conductivity of the solid nanoparticles, but also on their ability to remain dispersed over the observed short-term operating window. Qualitative macroscopic observations, as shown in Figure 4, suggest that low-frequency acoustic excitations play a role in temporarily mitigating macroscopic agglomeration.

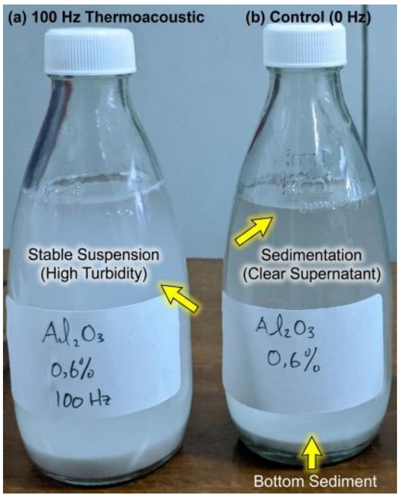


**Figure 4 Qualitative visual observation of 0.6% $Al_2O_3$ nanofluid after short-term testing: (left) with 100 Hz active low-frequency acoustic excitation, and (right) without acoustic treatment (control).**

While direct post-experimental micro-characterization (e.g., Zeta potential, dynamic light scattering, or UV-Vis absorbance) was not conducted within this macro-scale experimental scope, Figure 4 presents a qualitative macroscopic observation of the fluid state immediately following the short-term test. In the control sample (0 Hz), rapid macroscopic sedimentation occurs, likely due to uninhibited van der Waals attractive interactions among the 20–30 nm $\gamma$-$Al_2O_3$ particles, resulting in a clear supernatant and dense bottom sediment. Conversely, continuous low-frequency acoustic excitation, even at the lowest mechanical frequency of 100 Hz, appears to temporarily delay macroscopic settling and maintains higher visual turbidity without immediate visible sedimentation. This observation suggests that introducing supplemental mechanical energy across the 100 Hz–1000 Hz spectrum effectively stimulates the fluid medium. We hypothesize that this continuous low-frequency wave propagation produces localized acoustic streaming and oscillatory shear. This continuous forced mixing provides sufficient kinetic energy to counteract gravitational settling over the short-term operational duration without relying on chemical surfactants. However, we explicitly acknowledge that this visual inspection solely indicates a temporary delay in macroscopic settling. It cannot definitively establish absolute colloidal stabilization, which strictly requires rigorous quantitative verification. Despite these measurement limitations, the combined thermal enhancements and macroscopic stability observations suggest that low-frequency acoustic intervention offers a distinct operational paradigm compared to conventional methods. To contextualize the scientific contribution and practical implications of this current study, Table 2 presents a quantitative comparison between the proposed low-frequency acoustic technique and previously established nanofluid stabilization methods reported in the literature.

**Table 2 Comparison of the proposed low-frequency technique with previous experimental studies on $Al_2O_3$ nanofluids.**

| Reference | Stabilization Technique | Operating Conditions | Heat Transfer Enhancement | Key Limitations / Drawbacks |
|---|---|---|---|---|
| Poncet et al. (2022) | Low (25 kHz) and High (2 MHz) frequency ultrasound | Water, $Re$ = 890–14,500 | HTEF of 50% to 120% | Mechanical erosion risk at 25 kHz; 2 MHz enhancement drops to 0% at $Re >$ 7500. |
| Hedeshi et al. (2023) | High-frequency ultrasound (40 kHz) with $Al_2O_3$ nanofluid | $\phi$ = 0.4–0.8%, Flow rate = 113–257 L/h | Heat exchanger efficiency ratio increased up to 1.42 | Ultrasonic effectiveness is highly dependent on flow, diminishing significantly at higher flow rates. |
| Tahmasebi-Boldaji et al. (2023) | Ultrasonic probe and magnetic stirrer (surfactant-free) | $Al_2O_3$ ($\phi$ = 0.05–0.25%), pH = 3–11 | High short-term stability (zeta potential -32.8 mV) | Long-term sedimentation still occurs after 14 to 30 days. |
| Xiao et al. (2026) | Low-frequency strong sound waves (20–200 Hz) | Tube bundles, $Re$ = 150, SPL = 130–150 dB | Up to 4.19 times increase in local heat transfer | Requires extremely high sound pressure levels (>140 dB), posing severe equipment and spatial challenges. |
| Present Study | Low-Frequency Acoustic (1000 Hz) | $T_{mean}$ = 30.8–38.7°C, $Re \approx$ 21,000 | Max $h_o \approx 620$ $W/m^2 \cdot K$ | Requires long-term fouling and PEC validation |

As summarized in Table 2, while traditional high-frequency ultrasound achieves substantial thermal gains, it relies on inertial cavitation, which inherently carries the risk of internal pipe erosion. Similarly, chemical surfactants are effective but are limited by thermal degradation bounds. The proposed 1000 Hz low-frequency acoustic method presents a compelling alternative by providing sufficient macroscopic kinetic energy for forced mixing without crossing the threshold for destructive cavitation. Although the precise net energy benefits (PEC) and long-term fouling characteristics remain as limitations to be addressed in future work, this non-chemical approach establishes a promising baseline for environmentally benign industrial thermal management.

## Conclusions

Active low-frequency acoustic wave intervention was associated with observed short-term thermal changes, specifically enhancing the convective heat transfer performance of $Al_2O_3$ nanofluids in a counter-flow double-pipe heat exchanger. Nanofluid thermophysical properties are strongly influenced by nanoparticle concentration, with a 0.8% volume fraction yielding the highest convective heat transfer coefficient, reaching approximately 620 $W/m^2 \cdot K$ compared to 370 $W/m^2 \cdot K$ for the 0.2% concentration at 38.7°C. The introduction of continuous acoustic waves, particularly at the maximum tested frequency of 1000 Hz, is hypothesized to provide supplemental mechanical energy that induces acoustic streaming and forced mixing throughout the flow field. Visual inspections suggest that this acoustic agitation temporarily delays macroscopic particle sedimentation without requiring chemical surfactants.

However, these underlying mechanisms are currently treated as hypotheses. Furthermore, we explicitly acknowledge that long-term colloidal stability, non-destructive behavior on the heat exchanger walls, net energy benefits (e.g., comparing heat-transfer gain against speaker and pump electricity consumption), and overall industrial feasibility remain unverified in the current study. Future research must incorporate rigorous statistical testing across wider regimes, direct post-experimental micro-characterization (such as Zeta potential and dynamic light scattering), and extended multi-hour operational testing to comprehensively validate these preliminary findings. Beyond these empirical observations and current limitations, this study contributes to the broader thermal engineering field by establishing the fundamental concept of non-chemical, low-intensity mechanical agitation. Should the long-term scalability and net positive energy benefits be confirmed in future iterations, this non-destructive acoustic approach could pave the way for more sustainable, maintenance-friendly, and environmentally benign nanofluid thermal management systems across large-scale industrial applications.

## References

Ajeeb, W., da Silva, R. R. S. T., & Murshed, S. M. S. (2023). Experimental investigation of heat transfer performance of Al2O3 nanofluids in a compact plate heat exchanger. *Applied Thermal Engineering, 218*, 119321. 10.1016/j.applthermaleng.2022.119321

Azimy, H., Meghdadi Isfahani, A. H., & Farahnakian, M. (2022). Investigation of the effect of ultrasonic waves on heat transfer and nanofluid stability of MWCNTs in sono heat exchanger: an experimental study. *Heat and Mass Transfer, 58*(3), 467–479. https://doi.org/10.1007/s00231-021-03126-6

Brinkman, H. (1952) The Viscosity of Concentrated Suspensions and Solutions. The Journal of Chemical Physics, 20, 571-571. http://doi.org/10.1063/1.1700493

Dawar, A., & Cai, K. (2025). A thermal management algorithm for flow analysis of water-based Cu–Al2O3 hybrid nanofluid in multiple fields. *Engineering Applications of Computational Fluid Mechanics, 19*(1), 2591377. https://doi.org/10.1080/19942060.2025.2591377

Hedeshi, M., Jalali, A., Arabkoohsar, A., & Amiri Delouei, A. (2023). Nanofluid as the working fluid of an ultrasonic-assisted double-pipe counter-flow heat exchanger: M. Hedeshi et al. *Journal of Thermal Analysis and Calorimetry, 148*(16), 8579–8591. https://doi.org/10.1007/s10973-023-12102-7

Hou, J., Huang, L., Li, D., Zhao, X., Wei, N., Ma, L., Ding, Z., Chen, Z., Wei, J., & Hao, N. (2025). Acoustic-driven nanofluids for phase-change thermal management of electronic devices. *Journal of Colloid and Interface Science, 700*, 138368.

Kadhim, S. A., Abdul-Ghafoor, Q. J., Hammoodi, K. A., Abdul Wahhab, H. A., Ibrahim, O. A. A.-M., & Al-Ghezi, M. K. S. (2025). Enhancement of the heat transfer performance of a double-pipe heat exchangers in various configurations using $Al_2O_3$ nanofluid: a focused review. *Journal of Thermal Analysis and Calorimetry, 150*(6), 3941–3965. https://doi.org/10.1007/s10973-025-14042-w

Li, H., Wang, X., Li, Y., Wen, X., & Hu, Y. (2022). Effect of particle concentration on the flocculation and sedimentation of unstable Al2O3-SiO2/water hybrid nanofluid. *Journal of Nanoparticle Research, 24*(12), 263. https://doi.org/10.1007/s11051-022-05639-5

Maleki, N. M., Pourahmad, S., Khoshkhoo, R. H., & Ameri, M. (2023). Performance improvement of a double tube heat exchanger using novel electromagnetic vibration (EMV) method in the presence of Al2O3-water and CuO-water nanofluid; an experimental study. *Energy, 281*, 128193. https://doi.org/10.1016/j.energy.2023.128193

Maxwell, J. C. (1873). A treatise on electricity and magnetism (Vol. 1). Clarendon press.

Mostafa, H. A., Omran Osman, O., Abdelrhman, Y., Atef, M. M., & Ahmed, S. M. (2026). Optimizing sonication time for stable and efficient Al2O3-water nanofluid in direct solar absorption applications. *Particulate Science and Technology, 44*(2), 189–200. https://doi.org/10.1080/02726351.2025.2556021

Pak, B.C. and Cho, Y.I., (1998). Hydrodynamic and heat transfer study of dispersed fluids with submicron metallic oxide particles. *Experimental Heat Transfer an International Journal*, *11*(2), pp.151-170. https://doi.org/10.1080/08916159808946559

Poncet, C., Ferrouillat, S., Vignal, L., Courouble, A., Bulliard-Sauret, O., & Gondrexon, N. (2022). Ultrasonically enhanced convective heat transfer: Evidence of a relationship with the thermal boundary layer. *Applied Thermal Engineering, 216*, 119069. 10.1016/j.applthermaleng.2022.119069

Rahman, M. A., Hasnain, S. M. M., Pandey, S., Tapalova, A., Akylbekov, N., & Zairov, R. (2024). Review on nanofluids: preparation, properties, stability, and thermal performance augmentation in heat transfer applications. *ACS Omega, 9*(30), 32328–32349. https://doi.org/10.1021/acsomega.4c03279

Sonawane, S. S., & Malika, M. (2025). *Thermo-Acoustics of Nanofluids and Transfer Processes*. CRC Press.

Tahmasebi-Boldaji, R., Ghazanfari, S., Kuyakhi, H. R., Boldaji, N. T., & Torki, M. (2023). Experimental investigation of ultrasonic cycle/magnetic stirrer (UC/MS) effect on water/α-Al2O3 nanofluid stability and thermal conductivity and its ANFIS/PSO modeling. *Results in Engineering, 19*, 101284.
https://doi.org/10.1016/j.rineng.2023.101284

Xiao, C., Yang, Y., Liu, C., & Ouyang, Y. (2026). Low-frequency strong sound waves enhance heat transfer in tube bundles through acoustic streaming vortex formation. *Applied Thermal Engineering*, 132513. 10.1016/j.applthermaleng.2026.132513

Yasmin, H., Giwa, S. O., Noor, S., & Sharifpur, M. (2023). Thermal conductivity enhancement of metal oxide nanofluids: a critical review. *Nanomaterials, 13*(3), 597. https://doi.org/10.3390/nano13030597